Statistical Characteristics of Measured MIMO Wireless Channel Data and Comparison to Conventional Models

Jon W. Wallace and Michael A. Jensen
Department of Electrical and Computer Engineering
Brigham Young University, Provo, UT 84602-4099

Abstract— **This paper presents measured data from a narrowband multiple-input multiple-output (MIMO) channel probe in an indoor office/laboratory environment. The system employs ten transmit and ten receive antennas and computes the 10×10 narrowband channel matrix at 2.45 GHz every 80 milliseconds. We use the data to study the statistical behavior of the channel coefficients and the resulting channel capacity. We also demonstrate the ability of a simple statistically based physical model to accurately represent the channel behavior. The results of this model are compared to more conventional models that assume complex normal distributions of the channel matrix elements.**

I. Introduction

Recent studies have demonstrated the impressive theoretical capacity of wireless systems operating in a multipath environment and employing multiple antennas on both transmit and receive [1], [2]. In order to develop such multiple-input multiple-output (MIMO) systems, we must have accurate models that capture the complex spatial behavior of the propagation channel. In this paper, we discuss a measurement platform capable of directly measuring the MIMO narrowband channel matrix and show that a statistically based physical propagation model [3]-[4] matches capacity as well as joint magnitude and phase probability density functions of measured data for realistic model parameters. We compare the results of this model to more conventional models that assume complex normal distributions for the channel matrix elements. These comparisons show that as the numbers of antenna elements increases or the elements become more closely spaced, these simpler models are not able to fully characterize the channel behavior.

II. Measurement Platform

The experimental platform, depicted in Figure 1, uses a custom MIMO communications system operating at 2.45 GHz to directly measure the wireless MIMO channel transfer matrix $\mathbf{H}$, where $H_{mn}(\omega)$ represents the transfer function between the n^{th} transmitter and m^{th} receiver antennas [5]. The transmitter generates N unique binary (± 1) codes using a digital pattern generator and mixes them with a local oscillator to produce N distinct co-channel binary phase shift keyed (BPSK) signals. The resulting signals are amplified to 0.5 W and fed into one of the N transmit antennas.

The receiver amplifies and downconverts the signals from each of the M antennas. The resulting M intermediate frequency (IF) signals are low-pass filtered, amplified, and sampled using a 16-channel 1.25 Msample/s A/D card for storage on the PC. Two different antenna arrays have been constructed for the experiments. The first design is a 4-element dual-polarization patch array with half-wavelength element spacing. The second consists of a square metal plate with a two-dimensional grid of 33×33 holes spaced at roughly 1.5 cm intervals. Monopole antennas are placed in the holes to achieve a wide variety of array geometries.

The raw data collected using the measurement platform is processed to obtain estimates of the time-variant channel matrix. This processing first involves symbol timing recovery and carrier recovery stages to obtain synchronous complex baseband signals. A Maximum Likelihood algorithm is then used to estimate the channel matrix. For this study, the use of 1000-bit binary codes at a chip rate of 12.5 kbps produces an estimate of the channel every 80 ms.

This work was supported by the National Science Foundation under Wireless Initiative Grant CCR 99-79452 and Information Technology Research Grant CCR-0081476.

III. Measured Results

Table I lists the measurement parameters for the data sets under consideration in this study. Set 1 contains data from 5 different scenarios. In each scenario, the transmitter was fixed in one room while the receiver was moved to several different locations in another room. In set 2, a measurement was performed for every possible combination of 6 positions in one room for the receive array and 4 positions in a non-adjacent room for the transmit array. Both sets 1 and 2 exhibited rich multipath interference.

A. Normalization and Capacity

Obtaining a good statistical sample of the indoor channel requires collecting data in a variety of scenarios. Large movement in transmit and receive location leads to substantial change in the bulk signal path loss, potentially overshadowing interesting channel behavior such as signal spatial correlation. One way to remove this effect from collected data is to normalize the channel matrices.

Unless otherwise specified, channel matrices are normalized to force unit average single-input single-output (SISO) gain. The individual receiver noise is then given as $\sigma^2 = P_T/\text{SNR}$, where P_T is the total transmit power and SNR represents the desired signal-to-noise ratio at the receiver. This normaliza-

TABLE I
Data Set Parameters

Parameter	Set 1	Set 2
Antennas	4×4	10×10
Antenna Sep.	$\lambda/2$	$\lambda/4$
Antenna Type	Patch	Monopole
Polarization	V	V

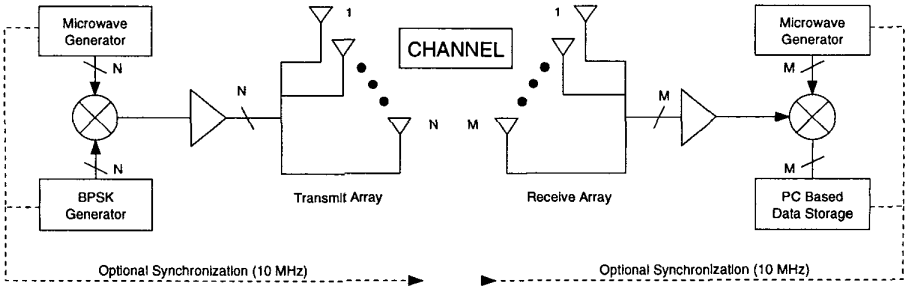

Fig. 1. High level system diagram of the narrowband wireless MIMO measurement system

tion is equivalent to specifying the average receiver SNR when transmit streams are uncorrelated. In this paper, the normalization constant is computed for each $\mathbf{H}$ matrix when computing capacity and over all $\mathbf{H}$ matrices at a single location for other quantities.

Capacity is computed by normalizing channel matrices to obtain an average SISO SNR of 20 dB. Capacity is computed using the water filling solution on the channel orthogonalized with the singular value decomposition (see [2]).

B. Joint PDFs

The complete joint probability density function (PDF) for all elements of the $\mathbf{H}$ matrix provides a complete statistical description of the narrowband MIMO channel. However, for large numbers of antennas the PDF dimensionality becomes prohibitive, and marginal PDFs or statistical moments must be used instead.

To allow comparison of measured and modeled channels, we use pairwise joint PDFs on magnitude and phase. We concentrate specifically on the statistics of adjacent elements at transmit and receive, since these will be the most correlated. The measured bivariate PDF for adjacent transmit/receive element magnitude is

$$f_{mP}(|x_1|,|x_2|) = \underset{\{i,j,k,\ell\}\in m_P}{\text{HIST2}}\,(|H_{ij}|,|H_{k\ell}|) \qquad (1)$$

where $P \in \{T,R\}$ for transmit or receive, $m_T = \{i,j,k,\ell : \ell = j+1, k = i\}$, $m_R = \{i,j,k,\ell : \ell = j, k = i+1\}$, and HIST2 is a two-dimensional normalized histogram operation. The measured univariate PDF for adjacent transmit/receive element phase difference is given as

$$f_{pP}(\Delta\phi) = \underset{\{i,j,k,\ell\}\in m_P}{\text{HIST}}\,[\arg(H_{k\ell}/H_{ij})] \qquad (2)$$

where HIST is a one-dimensional normalized histogram operation.

IV. Physical Channel Model

While measured data provides a comprehensive description of the channel behavior, simple models are highly desirable for assessing behavior of spatial multiplexing systems. Here, we propose an extension of the Saleh-Valenzuela model [3] that includes angle-of-arrival (AOA) statistics [4] to model the channel. Angle-of-departure (AOD) statistics are assumed to follow the same distribution as AOA, which is reasonable for the indoor channel with the same basic configuration on transmit and receive. The model is referred to here as the SVA model.

The SVA model characterizes the channel by representing each multipath component in terms of its amplitude, arrival time, and AOA/AOD. Based upon experimental observations, these arrivals or rays arrive in clusters in both space and time. Figure 2 shows the model parameters for a single cluster in the SVA model. The directional channel impulse response arising from L clusters and K rays per cluster is

$$\begin{aligned} h(\theta^R,\theta^T) &= \frac{1}{\sqrt{LK}}\sum_{\ell=0}^{L-1}\sum_{k=0}^{K-1}\beta_{k\ell}\delta(\theta^T-\Theta_\ell^T-\omega_{k\ell}^T) \\ &\quad\times\ \delta(\theta^R-\Theta_\ell^R-\omega_{k\ell}^R) \end{aligned} \qquad (3)$$

where θ^T and θ^R are the transmit and receive angle, $\beta_{k\ell}$ is the complex ray gain, Θ_ℓ^T and Θ_ℓ^R are the mean transmit and receive cluster arrival angles, and $\omega_{k\ell}^T$ and $\omega_{k\ell}^R$ are the relative angles of transmit and receive for the kth ray in the ℓth cluster.

To simplify the model for the narrow band channel, average ray power in each cluster is constant so that $\beta_{k\ell} \sim \mathcal{CN}(0,|\beta_\ell|^2)$, where $\mathcal{CN}$ denotes the complex normal distribution. The cluster amplitude is Rayleigh distributed with $\mathrm{E}\{|\beta_\ell|^2\} = \exp(-T_\ell/\Gamma)$. The arrival time distribution is a conditional exponential with a normalized unit arrival rate. Details concerning the model implementation can be found in [3]-[4]. The notation $\mathrm{SVA}(\Gamma,\sigma)$ is used in this paper to denote the SVA model with constant average ray power and unit cluster arrival rate, where Γ is the cluster decay constant and σ is the standard deviation of ray AOA/AOD.

The narrowband channel matrix is computed from the directional impulse response as

$$h_{mn} = \int_{2\pi}\int_{2\pi} W_m^R(\theta^R)h(\theta^R,\theta^T)W_n^T(\theta^T)d\theta^T d\theta^R \qquad (4)$$

where $W_q^P(\theta) = g_q^P(\theta)\exp[j\psi_q^P(\theta)]$, $g_q^P(\theta)$ is the antenna gain pattern, $\psi_q^P(\theta) = 2\pi[x_q^P\cos(\theta)+y_q^P\sin(\theta)]$, $P \in \{T,R\}$, and $q \in \{m,n\}$. Based upon measured data taken in [4], a two-sided Laplacian distribution is assumed for the ray AOA/AOD distribution whose PDF is

$$f^P(\omega) = \frac{1}{\sqrt{2}\sigma_P}\exp\left(-\left|\sqrt{2}\omega/\sigma_P\right|\right) \qquad (5)$$

where σ_P is the angular standard deviation.

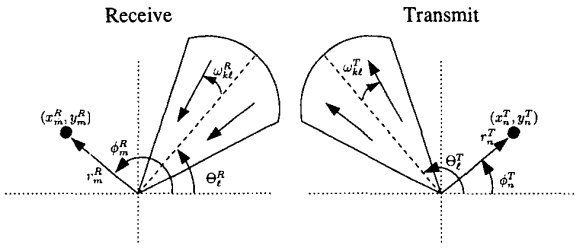

Fig. 2. Transmit and receive parameters for a single cluster in the SVA model.

A. Complex Normal Approximation

H matrices may be generated directly by computing (4) for each realization of the SVA model. An alternate method computes channel matrices according to a complex normal distribution for each fixed set of cluster statistics. This method reduces computational time and links the model to simpler complex normal models.

For a fixed set of cluster statistics (Θ_ℓ^T, Θ_ℓ^R, $|\beta_\ell|^2$) and ray arrival angles ($\omega_{k\ell}^T$, $\omega_{k\ell}^R$), h_{mn} is a weighted sum of zero mean complex normal random variables, resulting in a correlated complex normal distribution. If the angular spread on ω is small, the h_{mn} will look closely complex normal even if the $\omega_{k\ell}^P$ are allowed to vary. In this case, we find the average covariance matrix $\overline{\mathbf{R}}$ as

$$\begin{aligned}\overline{R}_{m_1n_1,m_2n_2} &= \mathrm{E}\{h_{m_1,n_1}h_{m_2,n_2}^*\} \\ &= \frac{1}{KL}\sum_{\ell_1=0}^{L-1}\sum_{\ell_2=0}^{L-1}\sum_{k_1=0}^{K-1}\sum_{k_2=0}^{K-1}\mathrm{E}\{\beta_{k_1\ell_1}\beta_{k_2\ell_2}^*\} \qquad (6) \\ &\times\ \mathrm{E}\{W_{m_1}^R(\Theta_{\ell_1}^R+\omega_{k_1\ell_1}^R)W_{m_2}^{R*}(\Theta_{\ell_2}^R+\omega_{k_2\ell_2}^R)\} \\ &\times\ \mathrm{E}\{W_{n_1}^T(\Theta_{\ell_1}^T+\omega_{k_1\ell_1}^T)W_{n_2}^{T*}(\Theta_{\ell_2}^T+\omega_{k_2\ell_2}^T)\}\end{aligned}$$

where statistical independence of complex ray gain, AOA, and AOD has been assumed. Further simplifications are possible if the gains of distinct rays are independent and ray AOA/AOD are i.i.d.

B. Comparison of Model and Data

Based upon high resolution AOA measurements [4], we begin with the key parameters $\sigma_{\{T,R\}} = 26°$, $\Gamma = 2$, $\Lambda = 1$. For simulation, transmit and receive cluster arrival angles are assumed to be uniform on $[0, 2\pi]$.

First, capacity PDFs and pairwise PDFs from the model are compared with measured 4 × 4 data from Set 1. Gain patterns for the antenna obtained from moment method simulations are used to compute the required covariance matrix. Figure 3 compares PDFs of measured data and Monte Carlo simulations of the SVA model. In these and later simulations, 10^5 channels were realized (100 cluster configurations with 1000 channels each). PDFs are computed for each cluster configuration, and these 100 functions are in turn averaged to obtain the results shown in the figures. Apparent in the figure is the good fit of both the capacity and pairwise amplitude PDFs. The discrepancy in phase is probably due to the fact that the uniform cluster AOA/AOD assumption is not strictly valid over the limited data set.

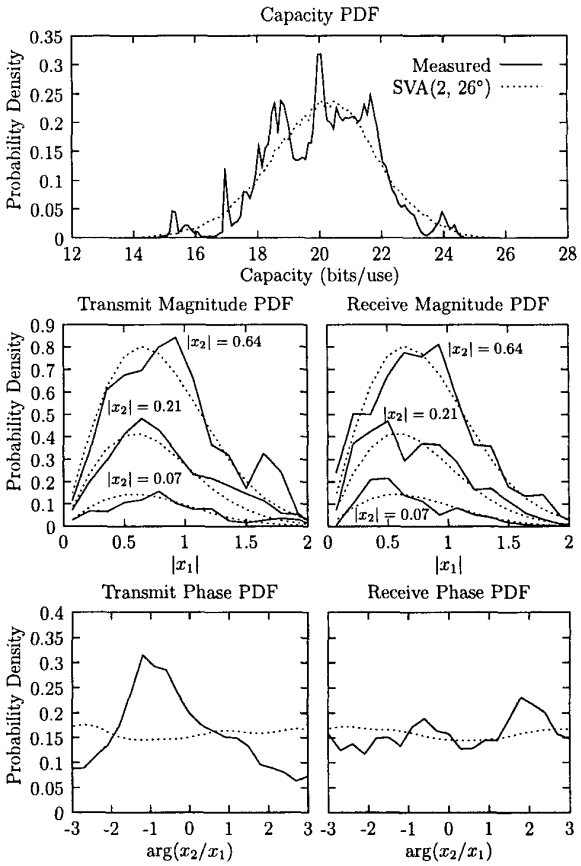

Fig. 3. Comparison of capacity PDFs and joint magnitude and phase PDFs for 4 × 4 measured data and SVA model simulations.

Next, capacity PDFs and pairwise PDFs from the model are compared with measured 10 × 10 data from Set 2. This data set employed quarter-wave monopole antennas, and an ideal uniform radiation pattern in azimuth was assumed. Figure 4 compares the PDFs for the measured and simulated 10 × 10 channel. While the parameters from [4] did not yield the desired fit for capacity, the figure shows that adjustment in either the cluster decay rate or angular ray spread improves the agreement. Detailed AOA/AOD measurements at the 2.4 GHz carrier are required to further study the discrepancy. Agreement in the amplitude and phase PDFs is comparable to the 4 × 4 data and does not change significantly with the parameter adjustments.

V. Other Channel Models

In many cases, it is assumed that underlying distribution on **H** is multivariate complex normal with covariance matrix obtained as the average covariance of the true distribution or $\mathbf{R} = \mathrm{E}\{\mathbf{h}\mathbf{h}^H\}$, where **h** is a stacked channel matrix. In other

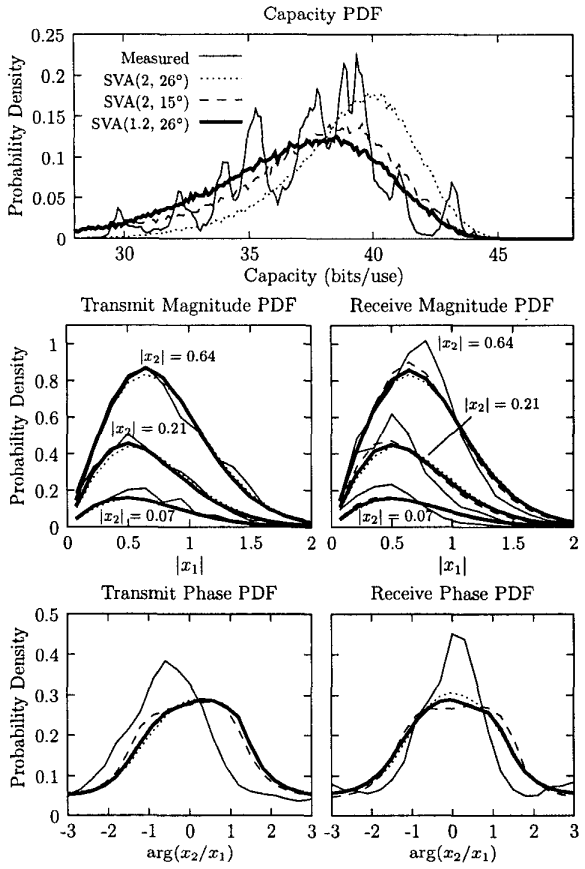

Fig. 4. Comparison of capacity PDFs and joint magnitude and phase PDFs for 10×10 measured data and SVA model simulations.

cases, the covariance matrix is assumed to be the elementwise square root of the power covariance matrix of the true $\mathbf{h}$ vector [6]. However, care is required since the root of the power covariance matrix is not necessarily positive definite. In this study, however, root power covariance matrices generated by the SVA model were always positive definite.

A. Simulation Results

Figure 5 plots capacity PDFs and the average pairwise magnitude and phase PDFs for simulated 4×4 channel matrices. Since the pairwise PDFs for transmit and receive look nearly identical, they have been averaged to obtain one plot for magnitude and another for phase. Linear arrays were assumed with $\lambda/2$ interelement spacing. Parameters for the SVA model were $\Gamma = 2$, $\sigma = 26°$, and uniform cluster AOA/AOD. The complex envelope method exhibits a good match for the pairwise PDFs but overestimates capacity. The power correlation model matches capacity PDFs and magnitude PDFs better at the cost of ignoring phase.

Figure 6 plots capacity PDFs and the average pairwise magnitude and phase PDFs for simulated 8×8 channel matrices

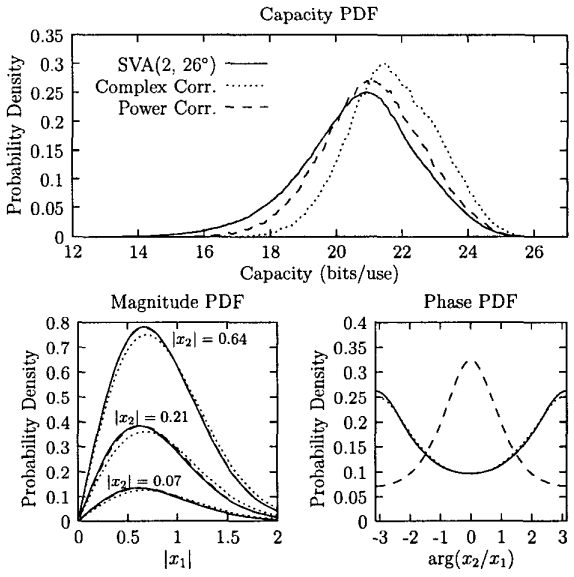

Fig. 5. Capacity PDFs and pairwise magnitude and phase PDFs for the 4×4 channel with $\lambda/2$ interelement spacing.

with $\lambda/2$ interelement spacing. The addition of antennas has apparently amplified the deficiencies present in the 4×4 case. Figure 7 shows the performance of the two methods for 8×8 arrays with an interelement spacing of $\lambda/4$. The complex envelope method performs about as well as for the $\lambda/2$ case. The power correlation method has great difficulty matching capacity, probably due to the significant correlation in phase which is ignored.

The simple models fail to match the SVA model because the covariance matrix is constant only for a fixed set of cluster statistics. Figure 8 demonstrates the random behavior of the covariance matrix by plotting the variance of the amplitude and phase of the elements of the correlation coefficient matrix generated with SVA model for the two 8×8 cases. Shift invariance of the model has been assumed so that the correlation coefficients are only a function of antenna separation at transmit and receive. For $\lambda/2$ separation, the element magnitudes (powers) and phases exhibit small and large variations respectively. Low power variance and highly random phase seem to be a good candidate for a power correlation model. For the $\lambda/4$ case, the power variation is more pronounced and the phases exhibit less variation. The poorer fit in capacity suggests that power models have difficulty in this case.

VI. Conclusions

This paper has explored the ability of a simple statistical model to capture key features of the narrowband indoor MIMO wireless channel. Ultimately, a tradeoff exists between model complexity and accuracy. However, we have shown that even simple models (like the SVA model), which are based partially on channel physics, match capacity and pairwise PDFs of measured data quite well. While simpler models based upon com-

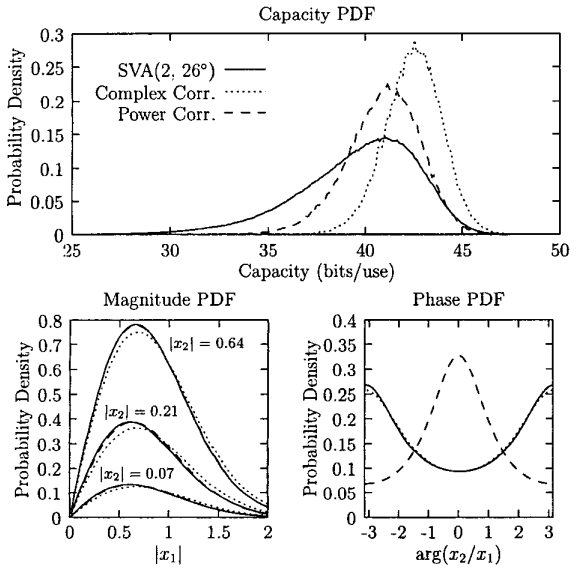

Fig. 6. Capacity PDF and pairwise magnitude and phase PDFs for 8 × 8 channel with $\lambda/2$ interelement spacing.

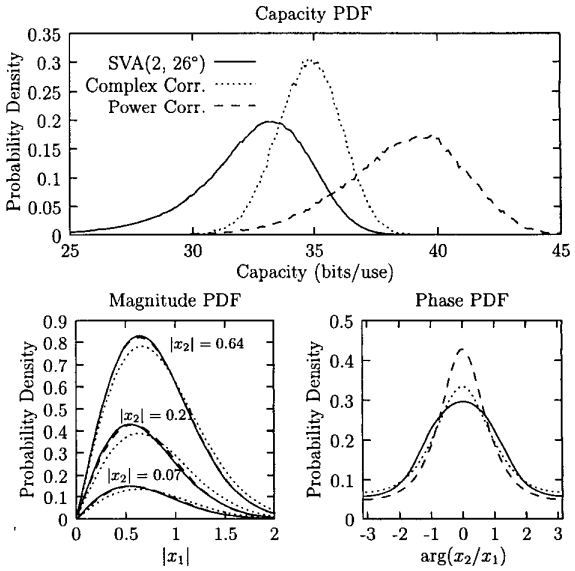

Fig. 7. Capacity PDF and pairwise magnitude and phase PDFs for the 8 × 8 channel with $\lambda/4$ interelement spacing.

plex normal distributions for the channel matrix elements are able to accurately predict capacity for certain scenarios, comparisons provided in the paper demonstrate that these models overpredict capacity as the number of antenna elements increases or the antenna spacing decreases, even when accurate covariance statistics are utilized in the random variable generation. This fact suggests that although the underlying statistical distribution of the channel matrix elements is marginally Gaussian, it may not be jointly Gaussian. Clearly, further research is required to adequately answer these fundamental questions concerning the MIMO wireless channel.

REFERENCES

[1] G. J. Foschini and M. J. Gans, "On limits of wireless communications in a fading environment when using multiple antennas," *Wireless Personal Communications*, vol. 6, no. 3, pp. 311–335, March 1998.

[2] Gregory G. Rayleigh and John. M. Cioffi, "Spatio-temporal coding for wireless communication," *IEEE Transactions on Communications*, vol. 46, no. 3, pp. 357–366, March 1998.

[3] Adel A. M. Saleh and Reinaldo A. Valenzuela, "A statistical model for indoor multipath propagation," *IEEE Journal on Selected Areas of Communications*, vol. SAC-5, pp. 128–13, February 1987.

[4] Q. Spencer, B. Jeffs, M. Jensen, and A. Swindlehurst, "Modeling the statistical time and angle of arrival characteristics of an indoor multipath channel," *IEEE J. Selected Areas Commun.*, vol. 18, no. 3, pp. 347–360, Mar. 2000.

[5] J. W. Wallace and M. A. Jensen, "Characteristics of measured 4x4 and 10x10 MIMO wireless channel data at 2.4-GHz," in *2001 IEEE Antennas and Propagation Intl. Symposium Digest (APS 2001)*, Boston, MA, July 2001, p. to appear.

[6] K. I. Pedersen, J. B. Andersen, J. P. Kermoal, and P. Mogensen, "A stochastic multiple-input-multiple-output radio channel model for evaluation of space-time coding algorithms," in *IEEE Vehicular Technology Conference (Fall VTC 2000)*, Boston, MA, Sep 2000, pp. 893–897.

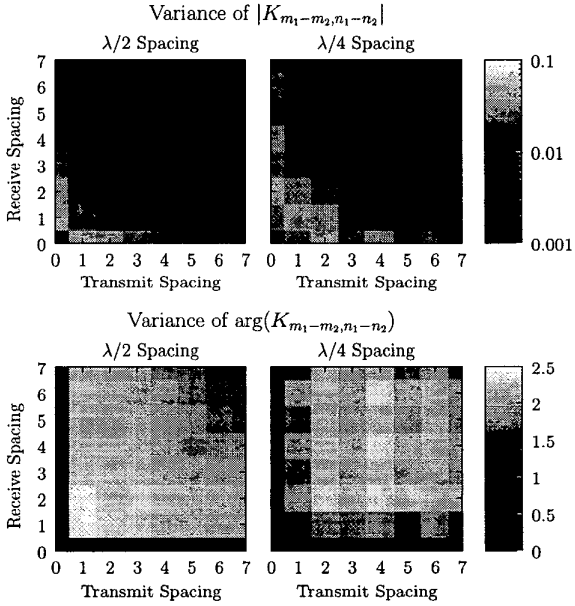

Fig. 8. Variance of the elements of the correlation coefficient matrix for the 8 × 8 channel data generated with the SVA model.